

Post-Cotunnite Phase of TeO₂

Gareth I. G. Griffiths and R. J. Needs

*Theory of Condensed Matter Group, Cavendish Laboratory,
J J Thomson Avenue, Cambridge CB3 0HE, United Kingdom*

Chris J. Pickard

*Department of Physics and Astronomy, University College London,
Gower St, London WC1E 6BT, United Kingdom*

(Dated: June 24, 2009)

We have used first-principles density-functional-theory methods with a random-structure-searching technique to determine the structure of the previously unidentified post-cotunnite phase of TeO₂. Our calculations indicate a transition from the cotunnite to post-cotunnite phase at 130 GPa. The predicted post-cotunnite structure has $P2_1/m$ space group symmetry and its calculated x-ray diffraction pattern is in good agreement with the available experimental data. We find that the cotunnite phase re-enters at about 260 GPa.

PACS numbers: 62.50.-p, 71.15.Nc, 61.50.-f, 91.60.Hg

INTRODUCTION

The majority of matter in the solar system is subject to pressures above 10 GPa,[1] which motivates studies of materials such as oxides at high pressures. In the case of AX_2 compounds, where A and X are, respectively, a divalent cation and halogen atom or a tetravalent cation and oxygen atom, the general effect of increasing the pressure is to distort the anion polyhedra and eventually to increase the coordination number (CN).[2] The highest CN observed in metal dioxides is in the PbCl₂-type cotunnite structure with CN=9. Metal dioxides with large cation radii often form cotunnite phases at high pressures, such as TiO₂, ZrO₂, HfO₂, CeO₂, PbO₂, PuO₂, UO₂, TbO₂, TeO₂,[3] and ThO₂. [4] The very important oxide SiO₂ is predicted to adopt the cotunnite structure above 690 GPa, which may be relevant to the study of extrasolar planets.[5] The hardest known oxide is the cotunnite structure of TiO₂, which has been synthesised at high pressures and recovered to ambient conditions.[6]

Materials that adopt the cotunnite structure are expected to transform under additional applied pressure into post-cotunnite structures with an accompanying increase in CN to 10 or more, as reported for some dihalides.[7] In reviewing the high pressure phases of dioxides our attention was drawn to TeO₂ which, to the best of our knowledge, is the only dioxide for which a transition to a post-cotunnite phase has been observed.[8] Sato *et al.*[8] studied TeO₂ up to pressures of 150 GPa in a diamond anvil cell. X-ray diffraction data showed strong evidence for a structural phase transition around 80-100 GPa, but the quality of the data was insufficient to allow a determination of the structure of the new phase, although the known post-cotunnite structures of dihalides were eliminated.[8] Identifying the post-cotunnite structure of TeO₂ would further our understanding of dioxides at high pressures.

TeO₂ is also an interesting material from the point of view of fundamental science and technology.[9] It has shown promise as a material for nonlinear optical devices, usually in a glassy form but potentially from nanosize crystals.[10, 11]

RANDOM STRUCTURE SEARCHING

First-principles or *Ab Initio* (AI) Density-Functional-Theory (DFT) methods have been widely applied to materials at high pressures, and have provided both confirmation of experimental results and predictions of new phases and their properties. DFT calculations have given very accurate descriptions of the high-pressure phases of *sp* bonded materials.[12] We have studied high-pressure phases of TeO₂ using AI DFT methods combined with “Random Structure Searching” (the AIRSS approach).[13] This approach has been used to predict high pressure phases which have subsequently been found experimentally,[13, 14] and to predict new high-pressure phases of materials such as hydrogen[15] and ammonia.[16]

The recipe for a random search commences by generating a set of initial structures, for each of which a random unit cell is created and renormalised to a reasonable volume, and the desired number of each atomic species is randomly distributed throughout. Each of these initial configurations is relaxed to a minimum in the enthalpy at a predefined pressure, and the procedure repeated until the lowest enthalpy structures have been found several times. Such random searching is largely unbiased, but it can often be made much more efficient by applying constraints. Any reasonable structure of TeO₂ will contain only Te-O bonds, and therefore we have performed most of the searches by placing O-Te-O molecules within the cells, rather than separate atoms. Another constraint we

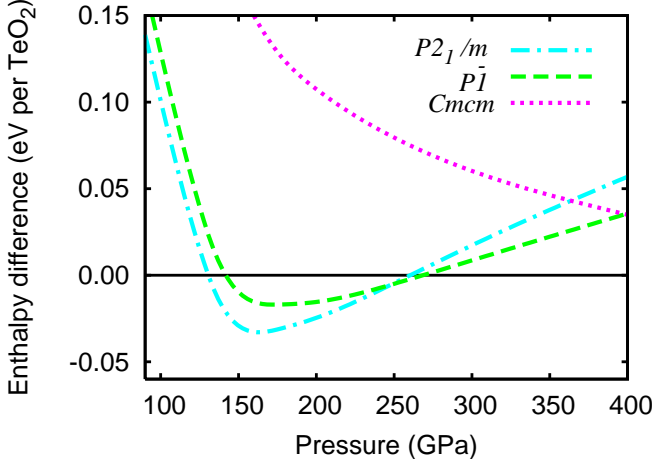


FIG. 1: (Color online) Enthalpy per TeO_2 unit relative to that of the cotunnite structure, as a function of pressure.

have employed is to reject initial configurations in which atoms are closer than a defined minimum separation. We have also generated initial configurations with the space groups which contain a specified number of symmetry operations, and then relaxed the structures while maintaining the symmetry.

Our DFT calculations were performed using the CASTEP[17] plane wave code with the Perdew-Burke-Ernzerhof (PBE) generalised gradient approximation (GGA) exchange-correlation functional[18] and ultrasoft pseudopotentials.[19] For the searches we used a plane wave cut off energy of 490 eV and a Monkhorst-Pack[20] Brillouin Zone sampling grid spacing of $2\pi \times 0.07 \text{ \AA}^{-1}$. All of the results reported in this paper were obtained by refining the structures obtained in the searches and calculating their properties using a higher level of accuracy consisting of a plane wave cut off energy of 800 eV and a grid spacing of $2\pi \times 0.03 \text{ \AA}^{-1}$.

We first performed searches at 150 GPa. Unconstrained searches were performed using 2 and 4 formula units of TeO_2 . Another set of searches was performed using initial configurations built by applying the symmetry operations of space groups chosen randomly from those with n operations to the randomly chosen positions of a Te atom and two O atoms, with $n = 3, 4, 6$ and 8 , all subject to a minimum separation of $r_{\min} = 1.3 \text{ \AA}$. Searches were then performed using O-Te-O molecules with initial bond angles of 120° , with 1, 2, and 3 molecular units and space groups with $n = 4$ operations, again with $r_{\min} = 1.3 \text{ \AA}$. Additional searches were performed at 280 GPa using molecules with initial bond angles of 120° . We used 1 molecular unit with $n = 4$ symmetry operations, 3 molecular units and $n = 2$ symmetry operations and $r_{\min} = 1.3 \text{ \AA}$, and 4 molecular units with $n = 2$ symmetry operations and $r_{\min} = 1.2 \text{ \AA}$. The searches produced a total of about 1800 relaxed structures.

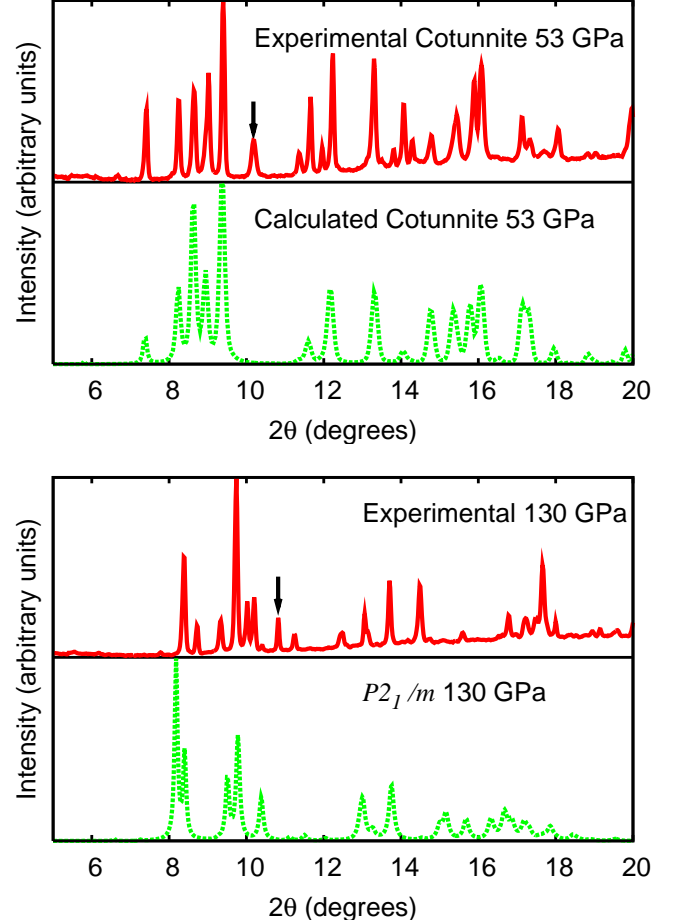


FIG. 2: (Color online) Comparison of observed (red solid lines) and calculated (green dashed lines) x-ray diffraction data for the cotunnite structure (upper box) at 53 GPa, and the $P2_1/m$ structure (lower box) at 130 GPa. The experimental diffraction data is from Ref. [8]. The experimental and calculated data were obtained with an x-ray wavelength of $\lambda = 0.4254 \text{ \AA}$. The black arrows mark known impurity lines in the experimental data,[8] although other impurity lines may also be present.

RESULTS FROM STRUCTURE SEARCHING

Enthalpy-pressure curves for the more stable phases are shown in Fig. 1. A structure of $P2_1/m$ symmetry was consistently the lowest enthalpy phase found at 150 GPa in all searches with a total of 4 formula units, and also in the 8 unit search with 2 symmetry operations applied to 4 molecular units. The structure with the second lowest enthalpy in these searches was always found to be the $Pnma$ cotunnite structure. Searches with 2 and 3 formula units did not yield structures with enthalpies as low as the searches with 4 or more, but a search with 6 formula units produced a low-symmetry $P\bar{1}$ structure which has an enthalpy between that of cotunnite and $P2_1/m$ at 150 GPa. The cotunnite, $P2_1/m$, $P\bar{1}$ and

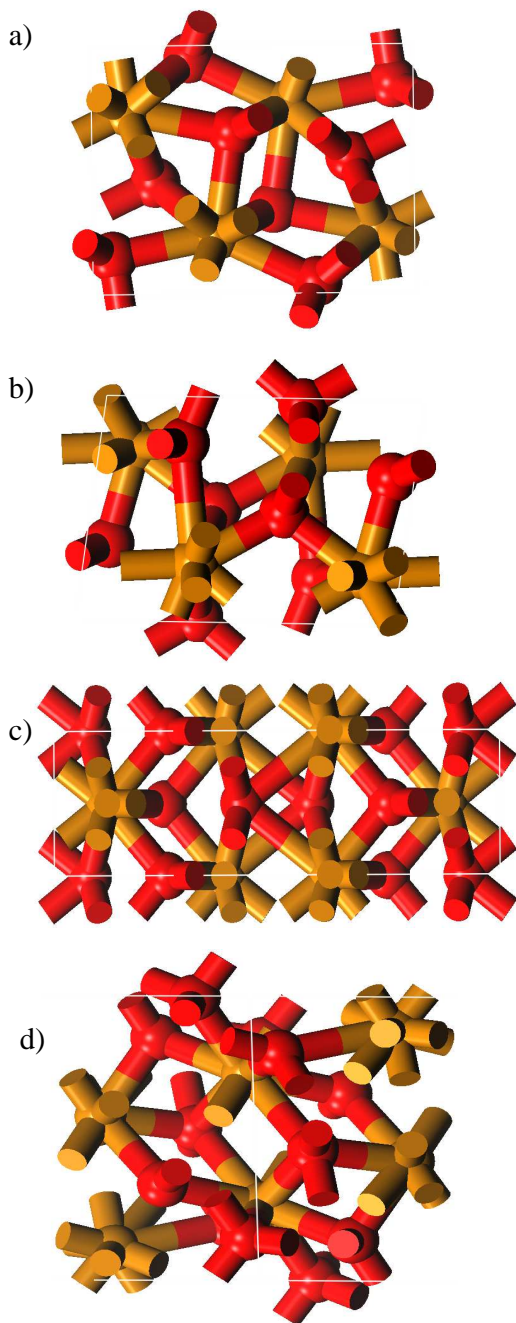


FIG. 3: (Color online) *a*) Cotunnite, *b*) $P2_1/m$, *c*) $Cmcm$ and *d*) $P\bar{1}$ structures. The yellow (light) spheres are Te atoms and the red (dark) spheres are O atoms.

$Cmcm$ structures are shown in Fig. 3 and their structural parameters are reported in Table I. The 12 unit search did not reveal any new structures that were lower in enthalpy than those already mentioned, although a previously unseen and fairly-low-enthalpy structure with space group $P2_1/c$ was found. The searches at 280 GPa did not yield any further low-enthalpy structures.

In our experience, the appearance of a very low sym-

metry structure, such as $P\bar{1}$, as a low enthalpy phase suggests that another structure of even lower enthalpy might exist. We therefore performed an additional type of search using the cell obtained by doubling that of $P\bar{1}$ in each direction, giving a cell containing 48 formula units. We then performed “shakes” of the larger structure in which all atoms were displaced in random directions by a distance chosen randomly between 0 and 0.25 Å, and then relaxed, but in each case the original $P\bar{1}$ structure was recovered.

The transition from cotunnite to $P2_1/m$ occurs at 130 GPa in our calculations. Sato *et al.* observed a phase transition at 80 GPa after heating the sample to 1000 K, and at 100 GPa at room temperature. Heating helps in overcoming kinetic barriers which are expected to be large in oxides and can also help to reduce anisotropic stresses. A temperature of 1000 K could, however, affect the coexistence pressure. The agreement between the measured transition pressure and the theoretical coexistence pressure is satisfactory, given the uncertainty in the experimental transition pressure and the fact that our calculations are at zero temperature. The maximum stabilization of the $P2_1/m$ phase over cotunnite is about 0.031 eV per TeO_2 unit at 175 GPa, which is quite small but easily resolved in our calculations. Such small enthalpy differences are often given quite accurately in DFT calculations for *sp* bonded materials where the volumes and the nature of the inter-atomic bonding in the two phases are very similar, as is the case here.

Fig. 1 shows that the $P\bar{1}$ structure is marginally the most stable in the pressure range 248–269 GPa, although the enthalpies of the $P\bar{1}$, $P2_1/m$, and cotunnite phases differ by less than 0.0023 eV per formula unit in this range. The cotunnite structure becomes more stable than the $P\bar{1}$ and $P2_1/m$ structures again at around 260 GPa. This re-entrant behavior of the cotunnite structure is quite unexpected. The origin of the apparent ‘kink’ in the enthalpies of the other structures relative to cotunnite in Fig. 1 actually lies with the nature of the cotunnite structure itself, as highlighted in Fig. 4. At pressures up to about 160 GPa, the compressibility of the cotunnite phase is nearly constant and is larger than that of $P2_1/m$, but at higher pressures the compressibilities are similar. The region of high compressibility of the cotunnite structure is predominantly associated with compression along the *a* axis, whilst the *c* axis actually increases in length from 125 to 150 GPa, before continuing to decrease steadily with increasing pressure. The cotunnite phase has a larger volume at pressures below about 160 GPa, but it is slightly smaller at higher pressures, which tends to favor cotunnite over $P2_1/m$.

The theoretical and experimental diffraction data for the cotunnite structure shown in Fig. 2 are in very good agreement. The discrepancies in relative peak heights might arise from the form factors used to generate the theoretical data, from the differences in structures due

Space group	Lattice parameters			Atomic coordinates			
	(Å, °)			(fractional)			
$Pnma$	$a=4.927$	$b=3.223$	$c=6.389$	Te1	0.2398	0.2500	0.6104
	$\alpha=90.00$	$\beta=90.00$	$\gamma=90.00$	O1	0.1536	0.2500	0.9378
				O2	0.0482	0.2500	0.3035
$P2_1/m$	$a=6.287$	$b=3.577$	$c=4.475$	Te1	0.1131	0.7500	0.2227
	$\alpha=90.00$	$\beta=97.15$	$\gamma=90.00$	Te2	0.3503	0.2500	0.7361
				O1	0.0711	0.7500	0.6543
				O2	0.2638	0.2500	0.2032
				O3	0.3930	0.7500	0.4901
				O4	0.3821	0.7500	0.9774
$Cmcm$	$a=3.014$	$b=10.144$	$c=3.232$	Te1	1.0000	0.8806	0.7500
	$\alpha=90.00$	$\beta=90.00$	$\gamma=90.00$	O1	1.0000	0.7527	0.2500
				O2	1.0000	0.5783	0.7500
$P\bar{1}$	$a=4.473$	$b=5.963$	$c=6.280$	Te1	0.1777	0.8322	0.1146
	$\alpha=99.95$	$\beta=97.56$	$\gamma=111.84$	Te2	0.5173	0.4923	0.2671
				Te3	0.8648	0.1658	0.4231
				O1	0.1107	0.1638	0.1524
				O2	0.0904	0.5140	0.3393
				O3	0.4251	0.1584	0.4611
				O4	0.6011	0.1671	0.1441
				O5	0.7083	0.8322	0.1993
				O6	0.7564	0.5003	0.0060

TABLE I: Structures of the cotunnite ($Pnma$, $Z = 4$ formula units per primitive cell), $P2_1/m$ ($Z = 4$ formula units per primitive cell), $P\bar{1}$ ($Z = 6$ formula units per primitive cell), and $Cmcm$ ($Z = 6$) phases of TeO_2 at 130 GPa.

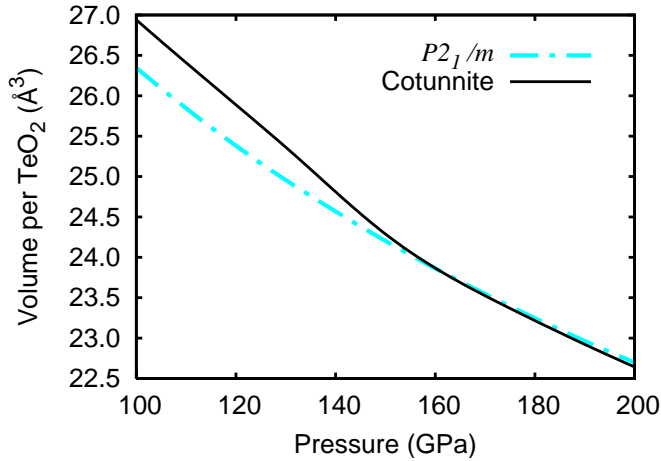


FIG. 4: (Color online) Volume per TeO_2 formula unit of the cotunnite and $P2_1/m$ structures.

to the approximate DFT and from the lack of temperature effects in the theoretical structure. The black arrow indicates an impurity line in the experimental data identified by Sato *et al.*, [8] which we see is absent in the theoretical data. The level of agreement between the theoretical and experimental x-ray data for the cotun-

nite phase gives us a benchmark for making a similar comparison for the post-cotunnite phase. The good level of agreement between the theoretical and experimental data for the post-cotunnite phase shown in Fig. 2 lends strong support to the viability of the $P2_1/m$ structure as a candidate for the post-cotunnite phase of TeO_2 . We note that the impurity line indicated by a black arrow in Fig. 2 for the post-cotunnite phase is absent in the theoretical data. Sato *et al.* [8] comment that other peaks in the experimental data may also be impurity lines, which could explain why some of the peaks are missing in the theoretical data.

The CN of the $Cmcm$ and $P2_1/m$ structures are both found to be ten, in comparison with cotunnite which has CN=9. The average of the nine nearest-neighbour Te-O distances in the cotunnite structure at 130 GPa is 2.16 Å with a range of 2.02–2.28 Å. For $P2_1/m$ the average is 2.23 Å with a significantly larger distribution of bond lengths of 1.98–2.99 Å. The $Cmcm$ structure has Te-O bond lengths of 2.02–2.51 Å with an average of 2.22 Å, slightly less than for $P2_1/m$ due to the smaller distortions of the oxygen polyhedra in $Cmcm$. The oxygen coordination numbers with respect to neighbouring Te atoms are 4 and 5 in cotunnite and 4 and 6 in $Cmcm$ and $P2_1/m$.

The $P2_1/m$ structure was studied in several other diox-

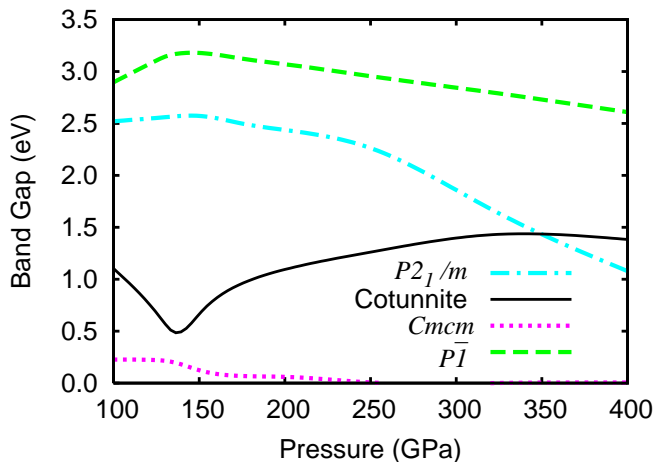


FIG. 5: (Color online) Band gaps of the cotunnite, $P2_1/m$, $Cmc m$ and $P\bar{1}$ structures as a function of pressure.

ides to establish whether it might be a more general post-cotunnite phase. TiO_2 , PoO_2 , ThO_2 , SeO_2 , SiO_2 , and HfO_2 were tested, but no evidence was found to suggest that $P2_1/m$ is more stable than cotunnite in any of these materials.

ELECTRONIC STRUCTURE OF THE PHASES

The pressure dependence of the calculated band gaps of the structures are shown in Fig. 5. Above about 135 GPa, the band gaps of the $P2_1/m$, $Cmc m$, and $P\bar{1}$ structures decrease with increasing pressure, however the cotunnite band gap unexpectedly begins to increase sharply from a minimum of 0.49 eV before levelling off at higher pressures. This kink in the pressure dependence of the band gap of cotunnite approximately coincides with the change in compressibility seen in Fig. 4. The band gap of the $Cmc m$ structure falls almost to zero by 250 GPa, although increasing the pressure further does not lead to overlapping valence and conduction bands. The insulating nature of the $P2_1/m$ phase is in agreement with the experimental observation of Sato *et al.*[8] that the material was not opaque up to the highest experimental pressure of 150 GPa.

The calculated band structures of the cotunnite and $P2_1/m$ phases at 130 GPa are shown in Fig. 6. The much larger band gap of the $P2_1/m$ phase is apparent. The eight lowest-energy bands for both phases arise from the $\text{O}2s$ states, and these lie at higher energies for the $P2_1/m$ structure, which has a somewhat smaller occupied bandwidth than cotunnite. Note that the band structure calculations were performed at the PBE-GGA level and are therefore expected to underestimate the true band gaps.

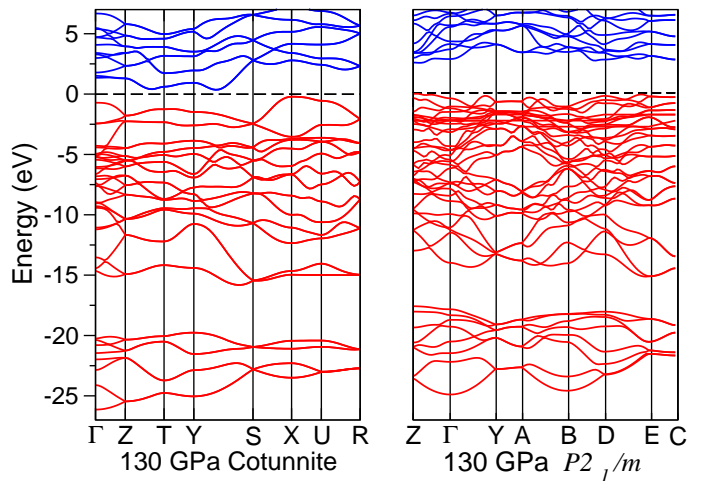


FIG. 6: (Color online) Band structures of the cotunnite (left) and $P2_1/m$ phases (right) at 130 GPa. The bands with energies below zero are occupied and those at higher energies are unoccupied.

CONCLUSIONS

We have searched for the post-cotunnite phase of TeO_2 using the AIRSS method. Our study supports the experimental observation of a post-cotunnite phase of TeO_2 at pressures readily accessible within a diamond anvil cell. We predict a transition to a tenfold coordinated $P2_1/m$ phase at 130 GPa (at zero temperature), for which the calculated x-ray diffraction data are in good agreement with experiment. Although the $P2_1/m$ phase has a smaller volume than the cotunnite phase up to about 160 GPa, cotunnite has a slightly smaller volume at higher pressures, and we predict that the cotunnite phase re-enters at about 260 GPa. The $P2_1/m$ phase does not appear to be a general post-cotunnite phase for the dioxides. The $P2_1/m$ phase is found to be an insulator over the range of pressures studied, up to 400 GPa, and hence should not appear opaque, in agreement with experiment.[8] Higher quality x-ray diffraction data are required to confirm whether our assignment of the $P2_1/m$ structure to the post-cotunnite phase of TeO_2 is correct.

ACKNOWLEDGEMENTS

This work was supported by the Engineering and Physical Research council (EPSRC) of the UK. Computational resources were provided by the Cambridge High Performance Computing Service. We thank the authors of Ref. [8] for providing their x-ray diffraction data in numerical form.

-
- [1] F. Manjon and D. Errandonea, *Phys. Status Solidi B* **246**, 1 (2009).
- [2] J. K. Dewhurst and J. E. Lowther, *Phys. Rev. B* **64**, 014104 (2001).
- [3] A. Jayaraman and G. A. Kourouklis, *J. Phys. Pramana* **36**, 2 (1991).
- [4] J. E. Lowther, *Phys. Rev. B* **72**, 172105 (2005).
- [5] K. Umemoto, R. M. Wentzcovitch, and P. B. Allen, *Science* **311**, 983 (2006).
- [6] L. S. Dubrovinsky, N. A. Dubrovinskaia, V. Swamy, J. Muscat, N. M. Harrison, R. Ahuja, B. Holm, and B. Johansson, *Nature* **410**, 653 (2001).
- [7] J. M. Leger, J. Haines, and A. Atouf, *J. Phys. Chem. Solids* **57**, 1 (1996).
- [8] T. Sato, N. Funamori, T. Yagi, and N. Miyajima, *Phys. Rev. B* **72**, 092101 (2005).
- [9] J.-C. Champarnaud-Mesjard, S. Blanchandin, P. Thomas, A. Mirgorodsky, T. Merle-Méjean, and B. Frit, *J. Phys. Chem. Solids* **61**, 9 (2000).
- [10] C. Lasbruggas, P. Thomas, O. Masson, V. Couderc, A. Barthélémy, and J.-C. Champarnaud-Mesjard, *J. Mat. Sci.* **40**, 4975 (2005).
- [11] S. Coste, A. Lecomte, P. Thomas, and J.-C. Champarnaud-Mesjard, *Langmuir* **24**, 21 (2008).
- [12] A. Mujica, A. Rubio, A. Muñoz, and R. J. Needs, *Rev. Mod. Phys.* **75**, 863 (2003).
- [13] C. J. Pickard and R. J. Needs, *Phys. Rev. Lett.* **97**, 045504 (2006).
- [14] C. J. Pickard and R. J. Needs, *Phys. Rev. B* **76**, 144114 (2007).
- [15] C. J. Pickard and R. J. Needs, *Nature Physics* **3**, 473 (2007).
- [16] C. J. Pickard and R. J. Needs, *Nature Materials* **7**, 775 (2008).
- [17] S. J. Clark, M. D. Segall, C. J. Pickard, P. J. Hasnip, M. I. J. Probert, K. Refson, and M. C. Payne, *Z. Kristallogr.* **220**, 567 (2005).
- [18] J. P. Perdew, K. Burke, and M. Ernzerhof, *Phys. Rev. Lett.* **77**, 3865 (1996).
- [19] D. Vanderbilt, *Phys. Rev. B* **41**, 7892 (1990).
- [20] H. J. Monkhorst and J. D. Pack, *Phys. Rev. B* **13**, 5188 (1976).